Progress in Oceanography 201 (2022) 102736

Contents lists available at ScienceDirect

Progress in Oceanography

journal homepage: www.elsevier.com/locate/pocean

Abundance and microbial diversity from surface to deep water layers over the Rio Grande Rise, South Atlantic

Juliana Correa Neiva Ferreira [1], Natascha Menezes Bergo [1,*], Pedro Marone Tura, Mateus Gustavo Chuqui, Frederico P. Brandini, Luigi Jovane, Vivian H. Pellizari

Instituto Oceanográfico, Universidade de São Paulo, São Paulo, Brazil

ARTICLE INFO

Keywords:
Picoplankton biomass
Microbial diversity
16S sequencing
Flow cytometry
Deep-sea mining
Rio Grande Rise

ABSTRACT

Marine microbes control the flux of matter and energy essential for life in the oceans. Until now, the distribution and diversity of planktonic microorganisms above Fe-Mn crusts have received relatively little attention. Future deep-sea mining is predicted to affect microbial diversity. Here, we studied the ecology of picoplankton among pelagic zones of a Fe-Mn deposit region, at Rio Grande Rise, Southwestern Atlantic Ocean. We investigated microbial community composition using high-throughput sequencing of 16S rRNA genes and their abundance estimated by flow cytometry.

The picoplankton populations were more abundant in epi- and mesopelagic waters, corresponding to the Tropical and South Atlantic Central Water masses. Bacterial groups related to heterotrophy, such as *Oceanospirillales* (Gammapoteobacteria), SAR11 (Alphapoteobacteria), *Flavobacteriales* (Bacteroida), and Rhodobacterales (Alphapoteobacteria), were the main representatives of the pelagic microbial community. Additionally, we detected abundant assemblages belonging to acetate-oxidizing manganese reducers, i.e., *Alteromonas*. No differences were observed in microbial community diversity among pelagic zones and water masses. These results provide the first insights into the picoplankton abundance, taxonomy and diversity, and ecological processes in the Rio Grande Rise of the Atlantic Ocean. This may also support draft regulations for deep-sea mining in the region.

1. Introduction

The world's oceans are an enormous pool of diverse microscopic life forms, which play a vital role in food chains and nutrient cycling (Teeling et al., 2012; Hogle et al., 2016). Marine picophytoplankton is responsible for almost half of the primary production on the planet, in particular, the genera *Synechococcus* and *Prochlorococcus* (Azam and Malfatti, 2007), capable of adsorbing trace metals from seawater for photosynthetic carbon fixation (Morel et al., 2020). Most of the particulate organic matter produced by the phytoplankton in the euphotic zone is excreted as dissolved organic matter which is remineralized by heterotrophic Bacteria and Archaea (Azam and Malfatti, 2007). A small fraction of the particulate organic carbon from primary producers is exported to deeper waters (Briggs et al., 2020), as the primary source of energy in and below the meso- and bathypelagic zones. This is particularly relevant to seamount and rise habitats and possibly those associated with ferromanganese (Fe-Mn) deposits due to their proximity to the productive zone above, a hydrodynamic setting which may increase the waters residence time (Genin and Dower, 2007), and microbial processes above seamounts (Mendonça et al., 2012; Lemos et al., 2018; Giljan et al., 2020).

The transport of organic matter produced in the euphotic zone to the benthic ecosystems adjacent to Fe-Mn deposits is relatively low (Smith et al., 2008; Wedding et al., 2013). Yet, it is an important source of bioactive metals (Smith et al., 2008; Wigham et al., 2003) and has a strong influence on benthic organisms and community diversity. Besides trace elements for enzyme cofactors, which catalyze key steps in respiration, nitrogen fixation, and photosynthesis, marine phytoplankton, and heterotrophic prokaryotes also require macronutrients for structural components such as proteins and membranes (Butler, 1998; Morel and Price, 2003).

Equally important, future Fe-Mn crust mining from seamounts is

* Corresponding author.
E-mail address: nataschabergo@gmail.com (N.M. Bergo).
[1] These authors contributed equally to this work.

https://doi.org/10.1016/j.pocean.2021.102736
Received 22 April 2021; Received in revised form 29 November 2021; Accepted 20 December 2021
Available online 24 December 2021

expected to physically alter the seafloor (Rolinski et al., 2001), producing a plume of waste material and impacting circulation, chemical characteristics, and redox potential of the adjacent water column (Orcutt et al., 2020). These changes may potentially alter the vertical transport of organic matter (Langenheder et al., 2010) and, consequently, the microbial contribution to the formation of Fe-Mn crusts (Orcutt et al., 2020). Although planktonic Bacteria and Archaea communities can rapidly respond to these environmental disturbances (Allison and Martiny, 2008), Orcutt et al. (2020) recommend that microbial diversity, biomass, and biogeochemical contributions need to be considered in environmental impact assessments of deep-sea mining.

In the present study, we investigate the planktonic microbial communities from the pelagic zones in the Rio Grande Rise (RGR). The RGR is a wide elevation (~150,000 km^2) located in the southwestern portion of the South Atlantic Ocean with complex morphology and water depth ranging from ~ 700 to 4000 m (Jovane et al., 2019). The RGR is within the oligotrophic Subtropical South Atlantic Gyre (Perez et al., 2012), under a regenerated production regime (*sensu* Dugdale and Goering, 1967; Metzler et al., 1997). The main reservoir of new nutrients is trapped below the permanent thermocline, in the South Atlantic Central Water (SACW), below the upper oligotrophic Tropical Water (TW) (Metzler et al., 1997). Deep chlorophyll maximum layer (DCM) is found ubiquitously (e.g., Jovane et al., 2019), and are the result of photoadaptation of picoautotrophs to low-light conditions rather than biomass accumulation, a typical tropical profile (*sensu* Cullen, 1982; Cullen, 2015).

The majority of the RGR is surrounded by the Antarctic Intermediate Water (AAIW), between 500 and 1000 m depth and characterized by the minimum water column salinity (approx. 34.2), and the Upper Circumpolar Deep Water (UCDW), between 1000 and 1300 m along with the minimum oxygen concentration, yet sufficiently high to favor aerobic reactions (approx. 4.1 ml l^{-1}, García-García et al., 2019; Silveira et al., 2020). Some RGR features, such as the central graben and external slopes, are occupied by the North Atlantic Deep Water (NADW). In general, west- southwest currents, usually around 5 cm s^{-1}, prevail over the RGR as part of the wind-driven and recirculation cells of the anticyclonic Subtropical Gyre in the upper and intermediate levels (Boebel et al., 1997; Stramma and England, 1999). However, intermittent and intense currents up to 50 cm s^{-1} were reported and related to tidal forcing and Tayllor columns over the complex RGR topography (Harlamov et al., 2015).

In the last decades, RGR is becoming strategic for potential mineral exploitation of Fe-Mn crusts (Montserrat et al., 2019; Benites et al. 2020; Bergo et al., 2021). However, the deep sea is turning into an official source of raw materials and it deserves environmentally sustainable management (Guilhon et al., 2021) that may only be achieved with biological studies.

This study aimed to describe planktonic microbial communities over the RGR water column, specifically by (1) the picoplanktonic abundance, (2) the diversity and composition of planktonic Bacteria and Archaea communities and (3) oceanographic features shaping microbial community composition. To achieve this, we sampled seawater from several stations across the RGR, and combined flow cytometry and next-generation sequencing.

2. Materials and methods

2.1. Sampling strategy

Seawater samples were collected at oceanographic stations along the RGR during the summer Marine E-Tech expedition (January - February 2018, more details in Jovane et al., 2019) onboard the R/V *Alpha Crucis* from the University of São Paulo (Fig. 1). Sampling depths per oceanographic station was defined according to the temperature (°C), salinity, oxygen (mg l^{-1}), fluorescent dissolved organic matter (*f*DOM, QSU), and phycoerythrin fluorescence (RFU) profiles provided by a combined Sea-Bird CTD/Carrousel 911 5 L Niskin rosette system, in order to sample the water masses.

Seawater (9L) was filtered using a peristaltic pump through 0.22 µm membrane pores (Sterivex, Millipore, MA) for molecular biology. Triplicate samples (1.5 ml) for flow cytometry were stored into cryovials and immediately preserved with Sigma-Aldrich glutaraldehyde solution (0.1% of final concentration), and flash-frozen in liquid nitrogen for a few minutes to fix. All samples for biological analysis were stored at –80 °C for up to 30 days until analysis. Samples for inorganic nutrients (nitrate, nitrite, phosphate, and silicate) were obtained from the filtered 0.22-µm water, stored at −20 °C, and determined on land by using a flow injection auto-analyzer (Auto-Analyzer 3, Seal *Inc.*). Additionally onboard, seawater (1-5L) from the TW and DCM was filtered using a vacuum pump through 0.7 µm fiberglass membrane (Whatman GF/F) and stored in liquid nitrogen for chlorophyll-a (CHL-a) measure. On land, fiberglass membrane were extracted with 90% acetone and

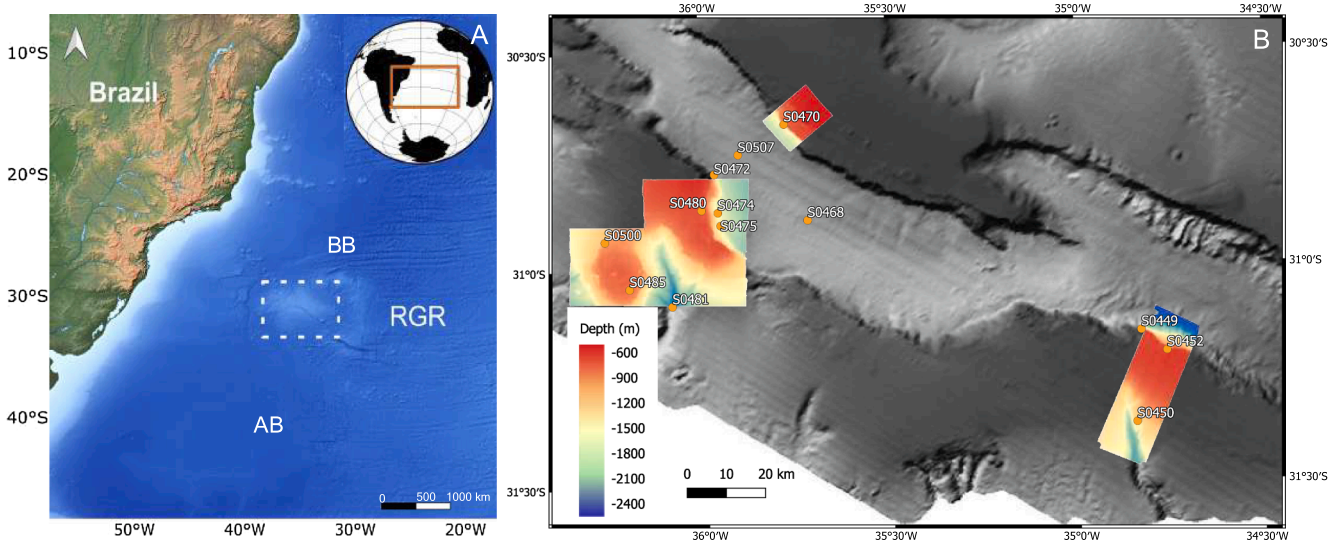

Fig. 1. (A) The sampling map with the location of Rio Grande Rise, South Atlantic Ocean. AB, Argentine Basin; BB, Brazilian Basin. (B) Distribution of oceanographic stations sampled in January - February 2018 (orange dots) across Rio Grande Rise. Numbers refer to stations. High resolution bathymetry (Jovane et al., 2019). (For interpretation of the references to colour in this figure legend, the reader is referred to the web version of this article.)

determined by using Turner 10AU fluorometer (Welschmeyer, 1994).

2.2. Flow cytometry analysis

Cell abundance of *Synechococcus* spp., *Prochlorococcus* spp., picoeukaryotes (≤2 μm), nanoeukaryotes (2–5 μm), and heterotrophic prokaryotes were determined according to Marie et al. (1999) using an Attune NxT flow cytometer (Thermo Fisher-Scientific) equipped with a syringe pump for quantitative volume sampling and two flat-top lasers: blue and red (488 nm e 640 nm respectively). Cells of *Prochlorococcus*, *Synechococcus*, picoeukaryotes, and nanoeukaryotes were quantified based on autofluorescence in red (BL3 - intracellular concentration of chlorophyll, 4.560 nm) and orange (BL2 - intracellular concentration of phycoerythrin, 530 ± 30 nm) wavelengths simultaneously. To reduce the noise, a threshold of 500 was applied to BL3. After analyzing the autotrophs, SYBR Green I (Invitrogen Life Technologies, USA) was added, and the samples were dark incubated at room temperature for 15 min (Marie et al., 1999). Flow cytometry acquisition for heterotrophic prokaryotes was triggered on BL1 (530 ± 30 nm) with a threshold value of 500 and 90° side scatter. Data were analyzed using Flowjo software® (https://www.flowjo.com/solutions/flowjo).

2.3. DNA extraction, 16S rRNA gene amplification, and Illumina MiSeq sequencing

DNA extraction was performed by using the DNeasy PowerWater (Qiagen, EUA) according to the manufacturer's instructions. Negative (no sample) extraction controls were used to ensure the extraction quality. DNA integrity was determined after electrophoresis in 1% (v/v) agarose gel prepared with TAE 1X (Tris 0.04 M, glacial acetic acid 1 M, EDTA 50 mM, pH 8), and staining with Sybr Green (Thermo Fisher Scientific, São Paulo, Brazil). DNA concentration was determined using the Qubit dsDNA HS assay kit (Thermo Fisher Scientific, São Paulo, Brazil), according to the manufacturer's instructions.

Before sending samples for preparation of Illumina libraries and sequencing, the V3 and V4 region of the 16S rRNA gene was amplified with the primer set 515F (5′–GTGCCAGCMGCCGCGGTAA-3′) and 926R (5′– CCGYCAATTYMTTTRAGTTT-3′), (Parada et al., 2016) to check for the amplification of 16S using the extracted DNA. Negative (no sample) extraction controls were used for PCR amplification and Illumina sequencing to check for the presence of possible environmental contamination (Sheik et al., 2018). Illumina DNA libraries and sequencing were performed at MR DNA (www.mrdnalab.com, Shallowater, TX, United States) on a MiSeq platform in a paired-end read run (2 × 250 bp) following the manufacturer's guidelines. Sequencing outputs were the raw sequence data.

2.4. Flow cytometry data and statistical analysis

Sampling maps and graphs of the hydrographic conditions of the water column and picoplankton carbon distribution for north stations were generated using Ocean Data View® with the DIVA gridding algorithm for variable resolution in a rectangular grid (Schlitzer, 2016). All data were used for statistical analyses with the R software (version 3.3.1).

Cell abundance was transformed (log(x + 1)) and non-metric multidimensional scaling (nMDS) using the Bray-Curtis similarity index was performed to look for patterns in the data. Environmental parameters were fitted to the nMDS using the envfit function of the vegan package with 999 permutations (Oksanen et al., 2016).

2.5. Sequencing data analysis, statistical analysis, and data visualization

The demultiplexed sequences were analyzed with the software package Quantitative Insights Into Microbial Ecology (QIIME 2) version 2019.4 (Bolyen et al., 2019) following the "Moving Pictures" tutorial (https://docs.qiime2.org/2018.8/tutorials/moving-pictures/). Sequences were denoised using DADA2 (Callahan et al., 2016) with the following parameters: trim left-f = 19, trim left-r = 18, trunc-len-f = 287, trunc-len-r = 215. Amplicon sequence variants (ASVs) with sequences of less than 10 occurrences were removed. The taxonomy was assigned to the representative sequences of ASVs using a Naive Bayes classifier pre-trained on SILVA release 132 clustered at 99% identity. FastTree and MAFFT (Katoh et al., 2013) were used to create a rooted phylogenetic tree which was used in calculating phylogenetic diversity metrics.

Diversity and phylogenetic analyses were performed with PhyloSeq (McMurdie and Holmes, 2012), ggplot2 (Wickham, 2009), and vegan (Oksanen et al. 2016) packages in the R software. Alpha-diversity metrics (e.g., Chao1 and Shannon diversity) were calculated based on ASV relative abundances for each sample. To determine if there were significant differences between alpha diversities, analysis of variance (Kruskal–Wallis one-way ANOVA on ranks test) test was performed in R. ASVs were normalized using the R package "DESeq2" by variance stabilizing transformation (Love et al., 2014). Beta diversity among pelagic zones and water masses was examined at an ordinated weighted Unifrac normalized distance and visualized using non-metric multidimensional scaling (nMDS, package Phyloseq). Multivariate Analysis of Variance (PERMANOVA) analysis to compare groups in the nMDS plots was performed with the adonis function in the R package vegan. Betadisper from the same package was used to assess the differences in dispersions between sample groups (Anderson, 2006).

Relative abundance of taxonomic indicators was identified by the IndicSpecies (Cáceres et al., 2010). The analysis was conducted on ASV counts excluding ASVS < 20 reads. We compared the relative abundance and relative frequency of each ASV to identify those specifically associated with only one water mass (unique) and those whose niche breadth encompasses several water masses (shared). The results were visualized as networks with the igraph R package (Csárdi and Tamas, 2006). Finally, to assess whether the 20 most abundant ASVs were associated with oceanographic features, Spearman rank correlation was calculated. A rho coefficient <0 indicates a negative correlation and a rho coefficient >0 a positive correlation. Raw sequence data generated for this are publicly available in the National Centre for Biotechnology Information (NCBI) database under the BioProject PRJNA714894.

3. Results

3.1. Water column and environmental factors

Seawater temperature ranged from 2 to 25 °C, with the coolest temperatures near the bottom at station 481, and the warmest temperatures in shallow waters at station 480 (Supplementary Fig. 1). Salinities ranged from 34.26 PSU at station 481 to 36 PSU at station 450 (Supplementary Fig. 1). Relatively lower temperatures and higher dissolved oxygen (>7 mg l^{-1}) were found associated with chl-a peaks (>0.3 μg l^{-1}). The DCM layer depth ranged from 80 to 150 m with chl-a values ranging from 0.28 μg l^{-1} at station 507 to 0.57 μg l^{-1} at station 480. Over surface layers and below the DCM, chl-a concentration was, in general, below 0.05 μg l^{-1} (Supplementary Table 1 and Supplementary Fig. 1).

The nutricline was also well-defined and coincident with or immediately adjacent to the SACW upper limit, except for nitrite (Supplementary Fig. 2). The vertical and spatial distribution of nitrate, phosphate, and silicate ranged between 0 and 42.94 μM, 0 and 3.1 μM, and 0.4 and 53.96 μM, respectively. High fDOM (>0.1 QSU) coincided with the presence of chl-a peaks at all stations. The fDOM varied between 0.02 and 0.19 QSU (Supplementary Table 1).

Stations representing the different pelagic zones and water masses were clearly distributed based on their environmental and physical characteristics in our PCA analysis (Supplementary Fig. 3). Three PCA components explained 83.03% of the sample variability based on

environmental parameters (temperature, salinity, oxygen, chl-a, nitrite, nitrate phosphate, silicate and fDOM). The first component (PC1) was negatively correlated with temperature and salinity and positively correlated with nitrate, which may reflect the influence of the cold and nutrient-rich SACW. The second axis (PC2) was negatively correlated with chl-a, while the third component (PC3) showed a high negative correlation with nitrite and a positive correlation with oxygen (Supplementary Table 2).

3.2. Pico- and nanoplankton abundance

Prochlorococcus corresponded to 72.4% of the total autotrophic cells (Supplementary Table 3 and Supplementary Table 4) and were dominant in the boundary between the TW and the SACW, ~100 m depth. The highest abundances were recorded at stations 485, 481, and 480, with 5.12×10^4, 4.82×10^4, and 4.3×10^4 cell ml^{-1}, respectively. Generally, in surface waters, few cells or no cells were recorded.

Synechococcus were more abundant in the surface layers, especially in the TW, in the upper 100 m. Maximum cell numbers were counted above DCM at all stations, and the highest abundances were recorded at 11 and 5 m depth in stations 475 and 507 (7.22×10^3 and 4.77×10^3 cell ml^{-1}, respectively). In general, *Synechococcus* abundance decreased with depth in all stations and corresponded to 18% of the total autotrophic cells (Supplementary Table 3 and Supplementary Table 4).

A similar vertical and spatial distribution was observed for photosynthetic picoeukaryotes and nanoeukaryotes. They were more abundant between 90 and 120 m depth in all stations. The maximum concentration (4.68×10^3 cell ml^{-1}, station 481) was found at 100 m depth, whereas lower abundance (<5.10×10^1 cell ml^{-1}) was recorded below 450 m. Picoeukaryotic populations corresponded to 9.4% of the total autotrophic cells (Supplementary Table 3 and Supplementary Table 4). Nanoeukaryotes were more abundant at stations 450 (9.3×10^2 cell ml^{-1}), 468 (8.61×10^2 cell ml^{-1}) and 449 (8.43×10^2 cell ml^{-1}). Higher cell concentrations were recorded at ca. 100 m. Nanoeukaryotes were (1.5%) the less abundant group of the total autotrophic cells (Supplementary Table 3 and Supplementary Table 4).

Heterotrophic prokaryotes dominated (averaging 99%) the microbial community (Supplementary Table 4). The higher abundances > 10^8 cell ml^{-1} occurred at southernmost stations 449 and 450 in the TW. Interestingly, heterotrophic prokaryotes concentration on other samples was four orders of magnitude lower, around 10^4 cell ml^{-1} (Supplementary Table 3 and Supplementary Table 4).

The spatial and vertical distribution of total picophytoplankton and heterotrophic prokaryotes were similar, with a higher abundance of both groups at the upper TW (Fig. 2F1 and F2). The higher picophytoplankton abundances were at stations 481, 485, 468, and 475, corresponding with the transition between TW and SACW.

Analyses using nMDS showed the picoplankton distribution over the pelagic zones, stations, and across environmental parameters, including temperature, salinity, chl-a, fDOM, and inorganic nutrients, as well as the water masses (Fig. 3). The biological groups correlated significantly with depth, temperature, salinity, oxygen, chl-a, and DCM ($p < 0.005$). The plankton community distribution was explained more by the pelagic zone (PERMANOVA, df = 2, F = 60, r^2 = 53%, p = 0.0009) than by the station (i.e., spatial distribution) (PERMANOVA, df = 1, F = 32, r^2 = 14%, p = 0. 0009).

3.3. Microbial alpha and beta diversity estimates

A total of 2,227,889 sequences were retrieved from 32 samples and ranged from 23,650 to 100,897 per sample. After removing chimeras, sequences were clustered into 3,628 amplicon sequence variants (ASVs) (0.03 cut-off). After filtering other contaminant groups, a total of 3,310 ASVs were obtained. Alpha diversity indices were not statistically different among the pelagic zones (Kruskal-Wallis one-way ANOVA, p > 0.005) (Supplementary Fig. 4). Microbial beta-diversity explored by ordinated weighted Unifrac normalized distance and ordered by nMDS did not reveal a clear distinction between epipelagic, meso- and bathypelagic samples (stress: 0.02; Supplementary Fig. 4). The analysis of variance with PERMANOVA showed that samples did not differ

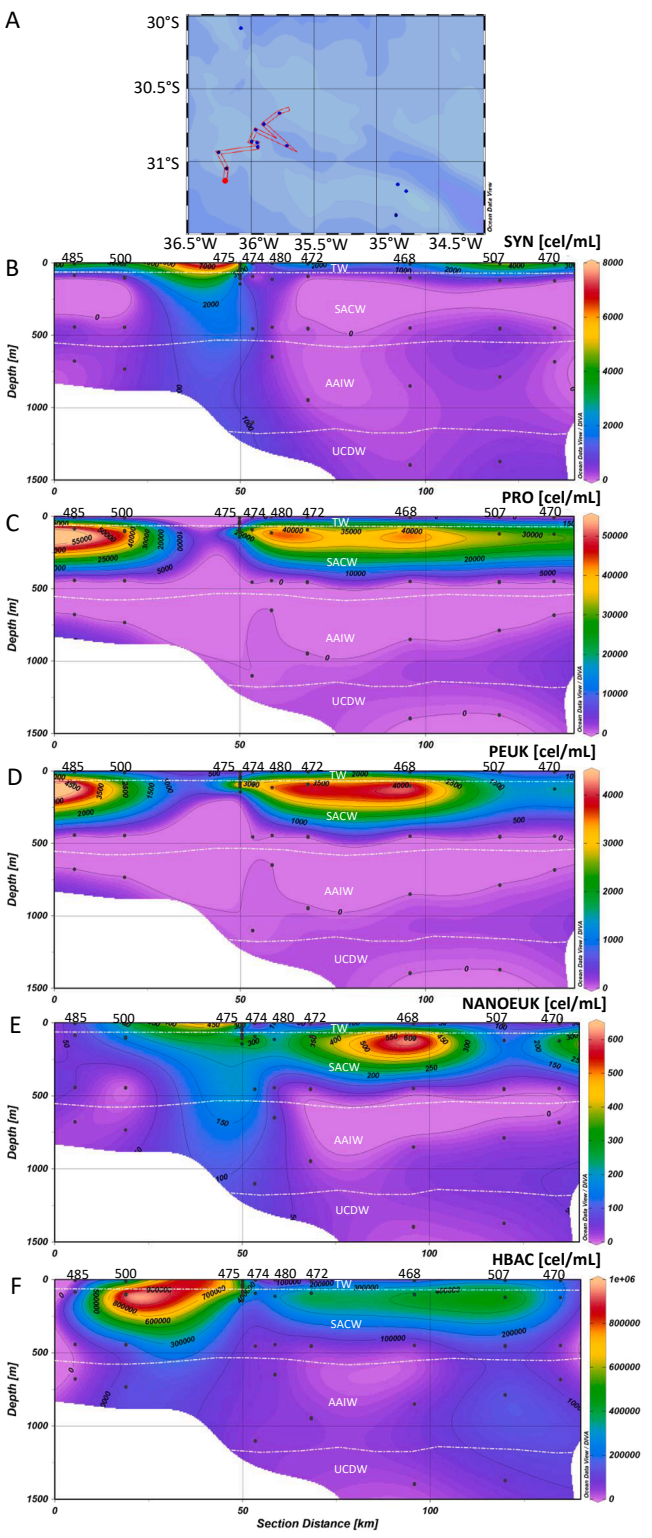

Fig. 2. Picoplankton abundance along the main sampling area in the Rio Grande Rise: (A) West stations, depth profiles of cells (cell mL ^{1}) distribution of (B) *Synechococcus* (Syn), (C) *Prochlorococcus* (Pro), (D) Picoeukaryotes (Peuk), (E) Heterotrophic bacteria (Hbac), and (F) Total Picophytoplankton. Additional stations to the east were also used for statistics.

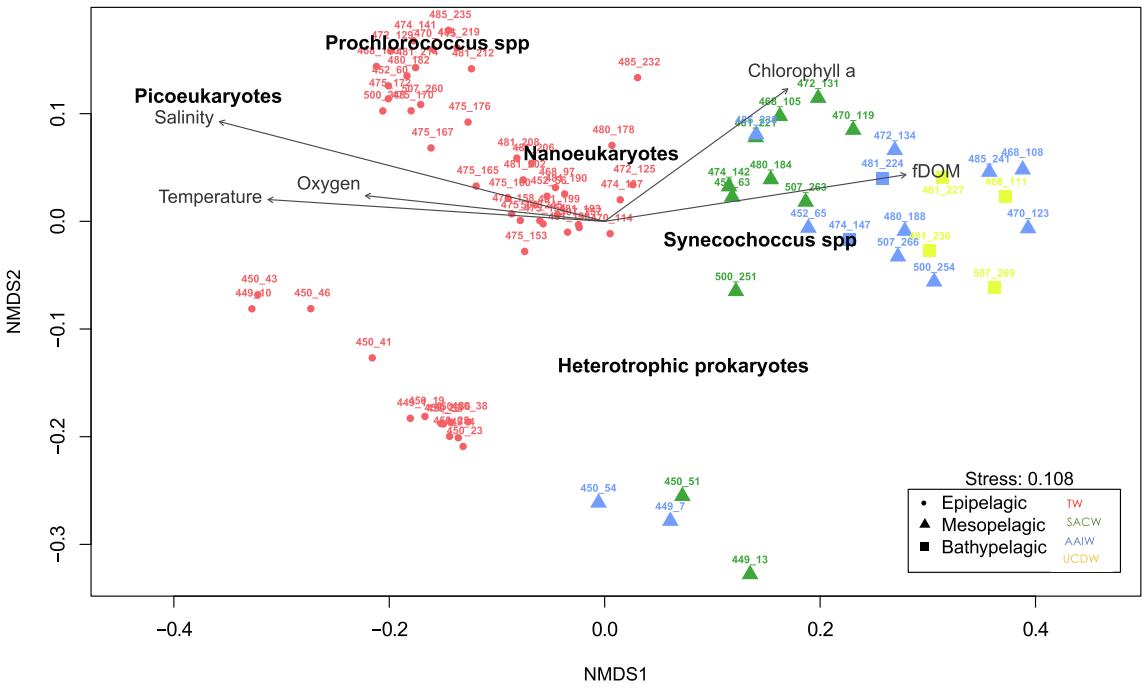

Fig. 3. Non-metric multidimensional scaling (nMDS) ordination of the Picoplankton abundance from the RGR (stress = 0.108). Circles represent samples collected in the epipelagic zone, triangles represent samples collected in the mesopelagic zone, and squares represent samples collected in the bathypelagic zone. Labels at samples represent stations. Different colors represent the water masses in the RGR: Red is Tropical Water (TW), green is South Atlantic Central Water (SACW), blue is Antarctic Intermediate Water (AAIW) and yellow is Upper Circumpolar Deep Water (UCDW). Each arrow shows one environmental gradient significantly correlated to the ordination (envfit, $p < 0.005$). The arrows point to the direction of the most rapid change in the environment (direction of the gradient) and its length is proportional to the correlation between ordination and environmental variable (strength of the gradient). (For interpretation of the references to colour in this figure legend, the reader is referred to the web version of this article.)

significantly when comparing pelagic zones, water masses, and depth (adonis, $p > 0.005$). Permuted analyses of beta-dispersion showed that samples did not differ significantly in the distance to the centroid (spread) among pelagic zones (betadisper, $p > 0.005$) and water masses (betadisper, $p > 0.005$).

3.4. Microbial community composition

The analysis of all sequences of the 16S rRNA gene showed that the communities were dominated by Bacteria (99.5%) rather than by Archaea (0.05%). At the phylum level, bacteria were dominated by Proteobacteria (33%, classes Gamma - and Alphaproteobacteria), Bacteroida (17%) and Actinobacteria, (5%) phyla. All archaeal communities

Fig. 4. Relative abundance of bacterial and archaeal taxonomic groups at the class level on the Rio Grande Rise. Only groups with more than 0.1% abundance are represented. Depths and sites of each sample are represented. Sequences were clustered at 97% similarity and taxonomy was assigned by performing BLAST searches against the Silva database v. 132 (*E*-value $\leq 1e{-}5$).

were dominated by Thaumarchaeota (*Nitrosopumilales*), followed by Euryarchaeota (*Marine Group*) (Fig. 4 and Supplementary Fig. 6).

Most taxonomic groups did not vary in abundance or occurrence between the pelagic zones, except for southernmost stations S0449 and S0450. For example, at the class level, the epipelagic zone (0–200 m) was dominated by Gammaproteobacteria (39.0%, order Oceanospirillales, Thimicrospirales, and Alteromonadales), Bacteroidia (28.5%, order Flavobacteriales), Alphaproteobacteria (24%, order SAR11_clade), Actinobacteria (2.2%, order Micrococcales), Nitrososphaeria (1.4%, order Nitrosopumilales) (Fig. 4). Whereas representatives of Cyanobacteriia (order Leptolyngbyales), Actinobacteria (order Micrococcales), NB1-j (order NB1-j), Nitrospiria (order Nitrospirales), and Nitrososphaeria (order Nitrosopumilales) were more abundant at the southernmost stations S0449 and S0450 (Fig. 5). In the mesopelagic zone, the prevalent classes were Gammaproteobacteria (38%, order Oceanospirillales, Thimicrospirales and Alteromonadales), Alphaproteobacteria (26.1%, order SAR11_clade), Bacteroidia (25%, order Flavobacteriales), Actinobacteria (2%, order Micrococcales), Nitrososphaeria (1.3%, order Nitrosopumilales) and Nitrospiria (0.9%, order Nitrospirales) (Fig. 5). Whereas classes that were more abundant in the southernmost station S0449 corresponded to Nitrospira (order Nitrospirales), NB1-j (order NB1-j), Nitrososphaeria (order Nitrosopumilales), and Actinobacteria (order Micrococcales (Fig. 5). The two samples from the bathypelagic zone (1000 m-4000 m) were dominated by ASVs affiliated to the Bacteroidia (33.5%, order Flavobacteriales), Gammaproteobacteria (32.8%, order Oceanospirillales, Thimicrospirales, and Alteromonadales), Alphaproteobacteria (32,3%, order SAR11_clade), Desulfobacteria (0.3%, order Desulfobacterales) and Fusobacteriia (0.2%, order) (Fig. 5).

Microbial community composition among different water masses was further investigated using the Indicator Species analysis (Fig. 5). We compared the relative abundance and relative frequency of each ASV to identify those specifically associated with only one water mass (unique) and those whose niche encompasses all water masses (shared). Only the water mass UCDW harbored a set of unique ASVs (n = 179) mainly belonged to the Flavobacteriales (n = 45), Chitinophagales (n = 17), Alteromonadales (n = 12), Bacteroidales (n = 8), Fusobacteriales (n = 5), Oceanospirillales (n = 5), Rhodobacterales (n = 5), Oceanospirillales (n = 5), Rhodobacterales (n = 5), Gammaproteobacteria_Incertae_Sedis (n = 4), JGI_0000069-P22 (n = 4), Cellvibrionales (n = 4) and Cytophagales (n = 4). The SACW and UCDW shared 1 ASV that was related to the Flavobacteriales order (Fig. 5).

3.5. Correlations between most abundant ASVs and oceanographic features

To identify key oceanographic features in shaping microbial community composition, Spearman correlations were calculated. Only bacterial ASVs (ASV1814, ASV1566, ASV2504 and ASV23160) showed a positive (rho > −0.5 or 0.5) and significant ($p < 0.05$) correlation with fluorescence (Supplementary Table 5).

4. Discussion

4.1. Distribution patterns of picoplankton and its link with physicochemical parameters

The complex water dynamics at seamounts and rises have been suggested to regulate spatial distributions and concentration of the picoplankton community (Mendonça et al., 2012; Milici et al., 2016; Giljan et al., 2020; Rocke et al., 2020). Picoeukaryotes dominated (>77%) the picophytoplankton across the RGR, as usually reported in the mesopelagic ecosystem (Agusti et al., 2015; Giner et al., 2020). They dominated in and below the DCM, mainly associated with the SACW,

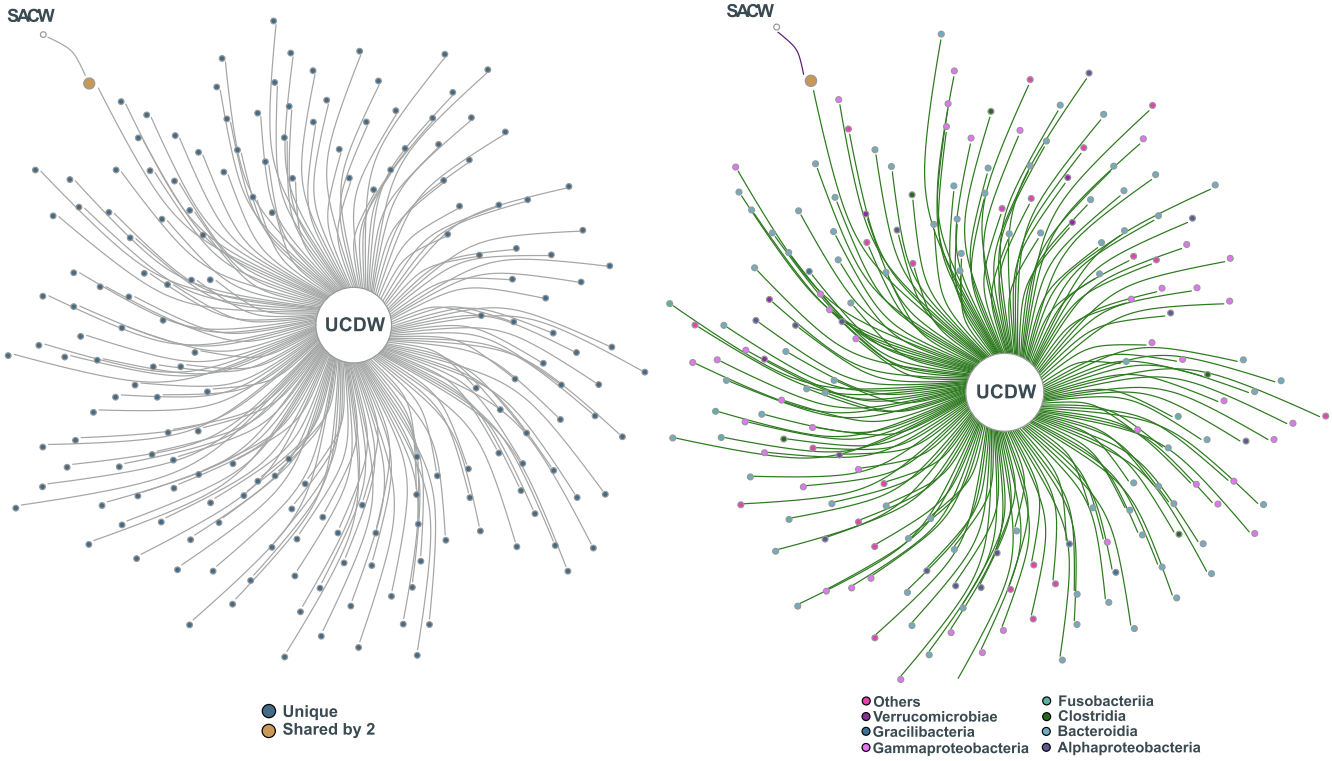

Fig. 5. Results of the Indicator Species analysis for water masses from RGR. The network (A) indicates the correlation (represented by edges) of unique and shared ASVs (between 2 different water masses presented as SACW - South Atlantic Central Water and UCDW - Upper Circumpolar Deep Water). The network (B) highlights the taxonomic classification of the nodes that belonged to the most represented orders (i.e., those representing >1% of relative abundance in at least one sample). Non-dominant taxa (i.e., < 1%) are reported as "Others". The size of the nodes reflects their "fidelity" to the substrates, so that a large node indicates those ASVs always present in all the samples of that water mass.

where nutrient availability, mainly nitrate and phosphate, is higher, as suggested by Pajares et al. (2019). The occasional detection of metabolically active and significant abundances of picoeukaryote groups in the dark ocean has been previously described (Agusti et al., 2015; Giner et al., 2020). This could be due to their attachment to sinking particles (Agusti et al., 2015) or migration in the water column in response to different gradients of light and nutrients to improve their growth conditions (Raven, 1998). Despite this, some picoeukaryotes may be mixotrophs (Faure et al., 2019). In this study, picoeukaryotes at and below the nutricline can be related to the resident populations that use nitrate from deeper waters (Bergo et al., 2017).

The abundance of *Prochlorococcus* was higher at ~100 m depth, close to the nutricline, which might indicate an ecotype adapted to low light intensity (Garcia-Robledo et al., 2017). In contrast, they were less abundant (sometimes even absent) in surface (<50 m) compared to other picophytoplankton groups. According to Lange et al. (2018), *Prochlorococcus* is expected to have the highest abundance within the picoautotrophs in oligotrophic waters, and we haven't confirmed this assumption yet. Previous studies have described that, low concentrations of photosynthetic pigments with the *Prochlorococcus* ecotypes in surface waters can lead to an underestimation of cell concentrations by the cytometer (Partensky et al., 1999; Gérikas Ribeiro et al., 2016a). Nevertheless, the observed mean cell concentrations were in the same order of magnitude as previous studies (Guo et al., 2014; Bergo et al., 2017), and this underestimation does not affect the spatial distribution patterns of picoplankton reported in this study. The abundance of *Synechococcus* was higher in the epipelagic zone, above the DCM associated with the relatively warm and nutrient-poor TW. Normally, the abundance of these cyanobacteria is lower in deep oceanic oligotrophic waters, decreasing with depth (Wang et al., 2011). Colder and nutrient-rich waters (including trace metals) inhibit *Synechococcus* growth (Wang et al., 2011).

Heterotrophic prokaryotes dominated the microbial community in the water column, with one order of magnitude more abundant than the other pico-sized groups, except for southernmost stations 449 and 450. Cotner and Wetzel (1992) suggest that heterotrophic prokaryotes dominate in oligotrophic waters in comparison to picophytoplankton. The related distribution between heterotrophic prokaryotes and picophytoplankton abundance in the water column reveals a connection among the picoplankton communities, the production of organic matter, and nutrient cycling in the RGR. This was expected particularly in the euphotic zone considering that the growth of heterotrophic prokaryotes is partially supported by dissolved organic compounds produced by phytoplankton cells, and the remineralization of inorganic nutrients by heterotrophic prokaryotes stimulates the phytoplankton growth (Linacre et al., 2015). Moreover, other sources of dissolved organic compounds may sustain the heterotrophic communities, for instance, viral lysis, seasonal blooms, and senescent cells (Buchan et al., 2014) which explains their dominance in deeper aphotic layers.

In general, the density of autotrophic and heterotrophic picoplankton populations was comparable to previous studies in the South Atlantic Ocean (Bergo et al., 2017; Gérikas Ribeiro et al., 2016a; Gérikas Ribeiro et al., 2016b). Excluding the heterotrophs, the *Prochlorococcus* dominated the autotrophic groups in our study (72.38%), followed by *Synechococcus* (16.77%), picoeukaryotes, and picoeukaryotes (9.39%). Besides photoadaptation by increasing the intracellular photosynthetic pigments, *Prochlorococcus* benefit from the small flux of nitrate (Berube et al., 2015) across the main pycnocline which explains their dominance among the picophytoplankton.

Although the abundance of the picoplankton varied vertically across sampling depths perhaps due to species-specific differences in photoadaptation and nutrient uptake efficiency, it also varied among stations, probably due to submesoscale (1–5 km) changes of turbulence and environmental conditions. The differences of microbial abundance and diversity among pelagic zones and water masses here observed, contribute to niche diversity and their spatial distribution.

4.2. Microbial community composition and diversity

Studies have shown that picoplankton bacteria and archaea diversity are structured by water masses (Agogué et al., 2011; Celussi et al., 2018), pelagic zones (Walsh et al., 2016), and depth (Mestre et al., 2017). Submarine mountains or elevations that divide the deep ocean into deep-oceanic basins may act as "ecological barriers" for prokaryotic communities (Salazar et al., 2016). However, our results showed no differences in bacterial and archaeal diversity among the pelagic zones, depth, and water masses in the Rio Grande Rise studied regions.

Microbial assemblages in the water column from the RGR showed the dominance of the classes Gammaproteobacteria and Alphaproteobacteria, within the Proteobacteria phylum, as described for other seamounts (Kato et al., 2018; Giljan et al., 2020) and the South Atlantic Ocean (Coutinho et al., 2020). The dominant bacterioplankton across the RGR consisted of heterotrophic members, i.e. *Oceanospirillales* and SAR11 Clade. *Oceanospirillales* have been described as associated with oil spills (Mason et al 2012; Cao et al., 2014) and symbiotic interactions with marine invertebrates (Verna et al., 2010). Whereas the SAR11 clade is the most abundant heterotrophic group in pelagic environments (Frank et al., 2016). Members of the SAR11 clade was well-established at marine oligotrophs regions with streamlined genomes and small cell sizes (Partensky et al. 1999; Giovannoni et al. 2017). Besides that, SAR11 has been suggested with high-affinity zinc and Fe ions uptake (Hogle et al., 2016). The dominance of SAR11 in the water column from RGR could be due to their capacity to respond to carbon limitation by metabolizing endogenous carbon (e.g. methane and methanol) in the dark and using proteorhodopsin to provide proton motive force in the photic zone (Giovannoni, 2017).

In addition to heterotrophic bacterioplankton, *Flavobacteriales* and Rhodobacterales groups were abundant in the RGR pelagic zone. Previous studies have shown that the order *Flavobacteriales* are the dominant group responding to phytoplankton blooms (Abell and Bowman, 2005; Teeling et al., 2012). This response consists of a succession of clades, namely NS9, NS4, NS2b, NS5, and Polaribacter, related to the colonization and consumption of phytoplankton-derived organic matter (Teeling et al., 2016; Unfried et al., 2018; Han et al., 2021). In our dataset, the relative abundance of the heterotrophic *Flavobacteriales* in seawater was significantly correlated with fluorescence ($rho > 0.50$, $p < 0.01$), suggesting that the availability of phytodetritus may be a key determinant for this group in the RGR. Besides that, members of Rhodobacterales (also referred to as Roseobacter) are also frequently found with relative abundance in response to changes in phytoplankton composition and after blooms (Zubkov et al., 2001; Rink et al., 2007; Isaac et al., 2021). Roseobacter contains isolates capable of dimethylsulfoniopropionate (DMSP) degradation (Wagner-Döbler and Biebl, 2006; Luo and Moran, 2015), an abundant organic sulfur compound produced by the phytoplankton. Also, this group has been associated with the utilization of low-molecular-weight dissolved organic carbon (Alonso-Sáez et al., 2007; Mayali et al., 2014) and organically complexed and inorganic metals (Hogle et al., 2016). Recently, members of Rhodobacteraceae contributed to the expression of genes involved in transport, sensing and regulation of Mo, Cd, Co, Cu, Ni, V, Zn, Mn, and Fe, indicating their prominent role in particulate trace element cycling (Debeljak et al., 2021).

The relative abundance of *Gammaproteobacteria* in the RGR increased with depth only at southern station 449, although it was reported previously for the North (Lauro and Bartlett, 2008) and South Atlantic Ocean (Coutinho et al., 2020). Within *Gammaproteobacteri*a, members of the order *Thiomicrospirales* and *Alteromonadales* (mostly represented by Colwelliaceae) were abundant in seawater in this study. Unexpectedly, *Thiomicrospirales* was detected at most of the stations in the RGR with a significant correlation with fluorescence ($rho = 0.56$, $p < 0.01$). Closely related sequences of *Thiomicrospirales* were reported previously only at oxygen minimum zones and hydrothermal vents (Meier et al., 2017; Pajares et al., 2020). Despite that, members of *Alteromonadales*, such as

Colwellia are suggested as the major contributing microorganisms in the dissolution of Mn in Fe–Mn crusts (Blöthe et al., 2015; Vandieken et al., 2012). In our results, we identified ASVs associated with acetate-oxidizing manganese reducers (Colwelliaceae) in all pelagic zones in most of the stations of the RGR.

Archaea is known to be an important component of the prokaryotic community in meso- and bathypelagic water masses in the oceans (Grzymski et al., 2012) and in the Fe-Mn deposits (Shulse et al., 2017; Kato et al, 2018). However, based on the recovered ASVs in this study, a low proportion of chemolithoautotrophic ammonia-oxidizing Archaea (Nitrososphaeria class) was detected in sea waters from RGR.

Recently, Bergo et al. (2021) recovered a high number of unclassified sequences from RGR samples. In fact, the indicator taxa for the deeper water mass UCDW reveals an unknown deep-sea environment influenced by unclassified and uncultured groups. Many of these taxa include the unclassified Gammaproteobacteria, uncultured and unclassified Flavobacteriaceae, and uncultured Rickettsiaceae and Saprospiraceae. In addition, the future mining/dredging of Fe–Mn crusts may change the physical structure of the seamount/rise and would potentially impact water circulation and biodiversity in the deep sea (Niner et al., 2018; Orcutt et al., 2020). These disturbances can consequently affect microbial ecology, functions still unknown, and biogeochemical and metal cycles in the Rio Grande Rise.

In conclusion, our results revealed that: (1) picoplankton niche diversity thrown depths and stations perhaps due to species-specific differences in photoadaptation, nutrient uptake efficiency, and oceanographic features; (2) microbial community diversity between pelagic zone and the water masses are no different; (3) the dominance of heterotrophic bacterioplankton in oligotrophic waters of the RGR, suggesting a higher phytoplankton-derived organic matter, (4) a high number of unclassified sequences were recovered from the RGR seawater, indicating an unknown species and hidden functions. Thus, further monitoring of the pelagic microbiome, such as metagenomics and metatranscriptome, measurement of the oceanographic conditions from the RGR, is needed to better elucidate the ecological processes and influence of pelagic microbiome in Fe-Mn crusts formation in the South Atlantic Ocean.

5. Availability of data and material

The sequencing reads generated for this study can be found in the National Centre for Biotechnology Information (NCBI) database under BioProject PRJNA714894.

Funding

This study was funded by the São Paulo Research Foundation (FAPESP), Grant number: 14/50820-7, Project Marine ferromanganese deposits: a major resource of E-Tech elements, which is an international collaboration between Natural Environment Research Council (NERC, United Kingdom) and FAPESP (Brazil). JCN received a scientific initiation scholarship from Programa Institucional de Bolsas de Iniciação Científica — CNPq/PIBIC (Process number 156954/2018-4). NMB was financed by a Doctoral fellowship from the *Coordenação de Aperfeiçoamento de Pessoal de Nível Superior* - Brasil (CAPES) - Finance Code 001. VHP and LJ are supported by FAPESP, grant number 18/17061-6.

CRediT authorship contribution statement

Juliana Correa Neiva Ferreira: Investigation, Methodology, Formal analysis, Visualization, Writing – original draft, Writing – review & editing. **Natascha Menezes Bergo:** Investigation, Methodology, Formal analysis, Visualization, Writing – original draft, Writing – review & editing. **Pedro Marone Tura:** Investigation, Writing – review & editing. **Mateus Gustavo Chuqui:** Methodology, Visualization, Formal analysis. **Frederico P. Brandini:** Project administration, Writing – review & editing. **Luigi Jovane:** Funding acquisition, Writing – review & editing. **Vivian H. Pellizari:** Supervision, Writing – original draft, Writing – review & editing.

Declaration of Competing Interest

The authors declare that they have no known competing financial interests or personal relationships that could have appeared to influence the work reported in this paper.

Acknowledgments

We are grateful to the captain and the crew of the Research Vessel Alpha Crucis, and scientists who joined the expedition Marine E-Tech RGR1 for their cooperation in sample collection. We would like to thank Linda Waters for the English language review. Sincere gratitude goes out to Carolina L. Viscarra and MSc. Mariana Benites for their scientific support on board. Also, a huge thanks to MSc. Mariana Benites for his help with plotting the sampling map. Concentrations of inorganic nutrients incorporated in this study were provided through the hard work of M.Sc Mayza Pompeu and Giulia Campos. A huge thank you to LECOM's research team and M.Sc Rosa C. Gamba for their scientific support.

Appendix A. Supplementary material

Supplementary data to this article can be found online at https://doi.org/10.1016/j.pocean.2021.102736.

References

Abell, G.C.J., Bowman, J.P., 2005. Colonization and community dynamics of class Flavobacteria on diatom detritus in experimental mesocosms based on Southern Ocean seawater. FEMS Microbiol. Ecol. 53 (2005), 379–391.

Anderson, M.J., 2006. Distance-based tests for homogeneity of multivariate dispersions. Biometrics 62, 245–253.

Agogué, Hélène, Lamy, Dominique, Neal, P.R., Sogin, M.L., Herndl, G.J., 2011. Water mass-specificity of bacterial communities in the North Atlantic revealed by massively parallel sequencing. Mol. Ecol. 20 (2), 258–274.

Agusti, S., González-Gordillo, J.I., Vaqué, D., Estrada, M., Cerezo, M.I., Salazar, G., Gasol, J.M., Duarte, C.M., 2015. Ubiquitous healthy diatoms in the deep sea confirm deep carbon injection by the biological pump. Nat. Commun. 6 (1) https://doi.org/10.1038/ncomms8608.

Allison, S.D., Martiny, J.B.H., 2008. Resistance, resilience, and redundancy in microbial communities. Proc. Natl. Acad. Sci. 105 (Supplement 1), 11512–11519.

Alonso-Sáez, L., et al., 2007. Bacterial assemblage structure and carbon metabolism along a productivity gradient in the NE Atlantic Ocean. Aquat. Microb. Ecol. 46 (1), 43–53.

Azam, F., Malfatti, F., 2007. Microbial structuring of marine ecosystems. Nat. Rev. Microbiol. 5 (10), 782–791.

Benites, M., Hein, J.R., Mizell, K., Blackburn, T., Jovane, L., 2020. Genesis and Evolution of Ferromanganese Crusts from the Summit of Rio Grande Rise, Southwest Atlantic Ocean. Minerals 10 (4), 349. https://doi.org/10.3390/min10040349.

Berube, P.M., Biller, S.J., Kent, A.G., Berta-Thompson, J.W., Roggensack, S.E., Roache-Johnson, K.H., Ackerman, M., Moore, L.R., Meisel, J.D., Sher, D., Thompson, L.R., Campbell, L., Martiny, A.C., Chisholm, S.W., 2015. Physiology and evolution of nitrate acquisition in Prochlorococcus. ISME J. 9 (5), 1195–1207.

Bergo, N.M., Bendia, A.G., Ferreira, J.C.N., et al., 2021. Microbial Diversity of Deep-Sea Ferromanganese Crust Field in the Rio Grande Rise, Southwestern Atlantic Ocean. Microb. Ecol.

Bergo, N.M., Signori, C.N., Amado, A.M., Brandini, F.P., Pellizari, V.H., 2017. The partitioning of Carbon biomass among the pico-and nano-plankton community in the South Brazilian Bight during a strong summer intrusion of South Atlantic central water. Front. Mar. Sci. 4 https://doi.org/10.3389/fmars.2017.00238.

Blöthe, M., et al., 2015. Manganese-cycling microbial communities inside deep-sea manganese nodules. Environ. Sci. Technol. 49 (13), 7692–7700.

Boebel, O., Schmid, C., Zenk, W., 1997. Flow and recirculation of Antarctic intermediate water across the Rio Grande rise. J. Geophys. Res.: Oceans 102 (C9), 20967–20986.

Briggs, N., Dall'Olmo, G., Claustre, H., 2020. Major role of particle fragmentation in regulating biological sequestration of CO2 by the oceans. Science 367 (6479), 791–793.

Bolyen, E., et al., 2019. "Reproducible, interactive, scalable and extensible microbiome data science using QIIME 2. Nat. Biotechnol. 37, 852–857.

Buchan, A., LeCleir, G.R., Gulvik, C.A., González, J.M., 2014. Master recyclers: features and functions of bacteria associated with phytoplankton blooms. Nat. Rev. Microbiol. 12 (10), 686–698.

Butler, A., 1998. Acquisition and utilization of transition metal ions by marine organisms. Science 281 (5374), 207–209.
Cao, Y., Chastain, et al., 2014. Novel psychropiezophilic Oceanospirillales species Profundimonas piezophile gen. nov., sp. nov., isolated from the deep-sea environment of the Puerto Rico trench. Appl. Environ. Microbiol. 80, 54–60.
Callahan, B.J., McMurdie, P.J., Rosen, M.J., Han, A.W., Johnson, A.J.A., Holmes, S.P., 2016. DADA2: High-resolution sample inference from Illumina amplicon data. Nat. Methods 13 (7), 581–583.
Celussi, M., Quero, G.M., Zoccarato, L., Franzo, A., Corinaldesi, C., Rastelli, E., Lo Martire, M., Galand, P.E., Ghiglione, J.-F., Chiggiato, J., Coluccelli, A., Russo, A., Pallavicini, A., Fonda Umani, S., Del Negro, P., Luna, G.M., 2018. Planktonic prokaryote and protist communities in a submarine canyon system in the Ligurian Sea (NW Mediterranean). Prog. Oceanogr. 168, 210–221.
James, B., Cotner Jr, Wetzel, Robert G., 1992. Uptake of dissolved inorganic and organic bphosphorus compounds by phytoplankton and bacterioplankton. Limnol. Oceanogr. 37 (2), 232–243.
Coutinho, F.H., von Meijenfeldt, F.A.B., Walter, J.M., Haro-Moreno, J.M., Lopéz-Pérez, M., van Verk, M.C., Thompson, C.C., Cosenza, C.A.N., Appolinario, L., Paranhos, R., Cabral, A., Dutilh, B.E., Thompson, F.L., 2020. Ecogenomics and metabolic potential of the South Atlantic Ocean microbiome. Sci. Total Environ. 765, 142758. https://doi.org/10.1016/j.scitotenv.2020.142758.
Csárdi, G., Tamas, N., 2006. The igraph software package for complex network research. Inter J. Complex Sys. 1695 (5), 1–9.
Cullen, J.J., 2015. Subsurface Chlorophyll Maximum Layers: Enduring Enigma or Mystery Solved? Annu. Rev. Mar. Sci. 7 (1), 207–239.
Debeljak, P., Blain, S., Bowie, A., Merwe, P., Bayer, B., Obernosterer, I., 2021. Homeostasis drives intense microbial trace metal processing on marine particles. Limnol. Oceanogr. 66 (10), 3842–3855.
Cullen, J.J., 1982. The deep chlorophyll maximum: comparing vertical profiles of chlorophyll a. Can. J. Fish. Aquat.Sci. 39 (5), 791–803.
De Cáceres, M., Legendre, P., Moretti, M., 2010. Improving indicator species analysis by combining groups of sites. Oikos 119 (10), 1674–1684.
Dugdale, R.C., Goering, J.J., 1967. Uptake of new and regenerated forms of nitrogen in primary productivity 1. Limnology and Oceanography 12 (2), 196–206.
Faure, E., Not, F., Benoiston, A.-S., Labadie, K., Bittner, L., Ayata, S.-D., 2019. Mixotrophic protists display contrasted biogeographies in the global ocean. ISME J. 13 (4), 1072–1083.
Frank, A.H., Garcia, J.A.L., Herndl, G.J., Reinthaler, T., 2016. Connectivity between surface and deep waters determines prokaryotic diversity in the North Atlantic Deep Water. Environ. Microbiol. 18 (6), 2052–2063.
Garcia-Robledo, E., Padilla, C.C., Aldunate, M., Stewart, F.J., Ulloa, O., Paulmier, A., Gregori, G., Revsbech, N.P., 2017. Cryptic oxygen cycling in anoxic marine zones. PNAS 114 (31), 8319–8324.
García-García, N., et al., 2019. Microdiversity ensures the maintenance of functional microbial communities under changing environmental conditions. ISME J. 13 (12), 2969–2983.
Gérikas-Ribeiro, C., dos Santos, A.L., Marie, D., Pellizari, V.H., Brandini, F.P., Vaulot, D., 2016a. Pico and nanoplankton abundance and carbon stocks along the Brazilian Bight. PeerJ 4, e2587.
Gérikas Ribeiro, C., Marie, D., Lopes dos Santos, A., Pereira Brandini, F., Vaulot, D., 2016b. Estimating microbial populations by flow cytometry, Comparison between instruments. Limnol. Oceanogr. Methods 14 (11), 750–758.
Giljan, G., Kamennaya, N.A., Otto, A., Becher, D., Ellrott, A., Meyer, V., Murton, B.J., Fuchs, B.M., Amann, R.I., Zubkov, M.V., 2020. Bacterioplankton reveal years-long retention of Atlantic deep-ocean water by the tropic Seamount. Sci. Rep. 10 (1) https://doi.org/10.1038/s41598-020-61417-0.
Giner, C.R., Pernice, M.C., Balagué, V., Duarte, C.M., Gasol, J.M., Logares, R., Massana, R., 2020. Marked changes in diversity and relative activity of picoeukaryotes with depth in the world ocean. ISME J. 14 (2), 437–449.
Genin, A., Dower, J.F., 2007. Seamounts: ecology, fisheries & conservation. In: Pitcher, Tony J. (Ed.), Blackwell Fish and Aquatic Resources Series. Blackwell Publishing, pp. 85–100.
Giovannoni, S.J., 2017. SAR11 Bacteria: The Most Abundant Plankton in the Oceans. Ann. Rev. Mar. Sci. 9 (1), 231–255.
Grzymski, J.J., Riesenfeld, C.S., Williams, T.J., Dussaq, A.M., Ducklow, H., Erickson, M., Cavicchioli, R., Murray, A.E., 2012. A metagenomic assessment of winter and summer bacterioplankton from Antarctica Peninsula coastal surface waters. ISME J. 6 (10), 1901–1915.
Guilhon, M., Montserrat, F., Turra, A., Link, J., 2021. Recognition of ecosystem-based management principles in key documents of the seabed mining regime: implications and further recommendations. ICES J. Mar. Sci. 78 (3), 884–899.
Guo, C., Liu, H., Zheng, L., Song, S., Chen, B., Huang, B., 2014. Seasonal and spatial patterns of picophytoplankton growth, grazing and distribution in the East China Sea. Biogeosciences 11 (7), 1847–1862.
Han, Y.u., Jiao, N., Zhang, Y., Zhang, F., He, C., Liang, X., Cai, R., Shi, Q., Tang, K., 2021. Opportunistic bacteria with reduced genomes are effective competitors for organic nitrogen compounds in coastal dinoflagellate blooms. Microbiome 9 (1). https://doi.org/10.1186/s40168-021-01022-z10.21203/rs.3.rs-969333/v1.
Harlamov, V., et al., 2015. Preliminary results onmid-depth circulation features on Rio Grande Rise. In: 2015 IEEE/OES Acoustics in Underwater Geosciences Symposium (RIO Acoustics). IEEE.
Hogle, S.L., Thrash, J.C., Dupont, C.L., Barbeau, K.A., Müller, V., 2016. Trace Metal Acquisition by Marine Heterotrophic Bacterioplankton with Contrasting Trophic Strategies. Appl. Environ. Microbiol. 82 (5), 1613–1624.
Isaac, A., et al., 2021. Tight Adherence (Tad) Pilus Genes Indicate Putative Niche Differentiation in Phytoplankton Bloom Associated Rhodobacterales. Front. Microbiol. 12.
Jovane, Luigi, et al., 2019. Multidisciplinary scientific cruise to the Rio Grande Rise. Front. Mar. Sci. 6, 252.
Kato, S., Okumura, T., Uematsu, K., Hirai, M., Iijima, K., Usui, A., Suzuki, K., 2018. Heterogeneity of Microbial Communities on Deep-Sea Ferromanganese Crusts in the Takuyo-Daigo Seamount. Microbes Environ. 33 (4), 366–377.
Katoh, K., et al., 2013. MAFFT multiple sequence alignment software ver. 7: improvements in performance and usability. Mol. Biol. Evol. 30, 772–780.
Lange, P., Brewin, R., Dall'Olmo, G., Tarran, G., Sathyendranath, S., Zubkov, M., Bouman, H., 2018. Scratching beneath the surface: A model to predict the vertical distribution of Prochlorococcus using remote sensing. Remote Sens. 10 (6), 847. https://doi.org/10.3390/rs10060847.
Langenheder, Silke, et al., 2010. "Bacterial biodiversity-ecosystem functioning relations are modified by environmental complexity. PloS One 5 (5), e10834.
Lauro, F.M., Bartlett, D.H., 2008. Prokaryotic lifestyles in deep sea habitats. Extremophiles 12 (1), 15–25.
Lemos, A.T., Ghisolfi, R.D.R., Mazzini, P.L.F., 2018. Annual phytoplankton blooming using satellite-derived chlorophyll-a data around the Vitória-Trindade Chain, Southeastern Brazil. Deep Sea Res. Part I: Oceanographic Res. Pap. 136, 62–71.
Linacre, L., Lara-Lara, R., Camacho-Ibar, V., Herguera, J.C., Bazán-Guzmán, C., Ferreira-Bartrina, V., 2015. Distribution pattern of picoplankton carbon biomass linked to mesoscale dynamics in the southern gulf of Mexico during winter conditions. Deep Sea Res. Part I: Oceanographic Res. Pap. 106, 55–67.
Love, M.I., Huber, W., Anders, S., 2014. Moderated estimation of fold change and dispersion for RNA-seq data with DESeq2. Genome Biol. 15 (12) https://doi.org/10.1186/s13059-014-0550-8.
Luo, H., Moran, M.A., 2015. How do divergent ecological strategies emerge among marine bacterioplankton lineages? Trends Microbiol. 23 (9), 577–584.
Mason, O.U., Hazen, T.C., Borglin, S., Chain, P.S.G., Dubinsky, E.A., Fortney, J.L., Han, J., Holman, H.-Y., Hultman, J., Lamendella, R., Mackelprang, R., Malfatti, S., Tom, L.M., Tringe, S.G., Woyke, T., Zhou, J., Rubin, E.M., Jansson, J.K., 2012. "Metagenome, metatranscriptome and single-cell sequencing reveal microbial response to Deepwater Horizon oil spill. ISME J. 6 (9), 1715–1727.
Meier, D.V., Pjevac, P., Bach, W., Hourdez, S., Girguis, P.R., Vidoudez, C., Amann, R., Meyerdierks, A., 2017. Niche partitioning of diverse sulfur-oxidizing bacteria at hydrothermal vents. ISME J. 11 (7), 1545–1558.
Mendonça, Ana, et al., 2012. Is There a Seamount Effect on Microbial Community Structure and Biomass? The Case Study of Seine and Sedlo Seamounts (Northeast Atlantic). PLOS ONE 18.
Mestre, M., Borrull, E., Sala, M.M., Gasol, J.M., 2017. Patterns of bacterial diversity in the marine planktonic particulate matter continuum. ISME J. 11 (4), 999–1010.
Marie, D., Brussaard, C., Partensky, F., Vaulot, D., Wiley, J., 1999. Flow cytometric analysis of phytoplankton, bacteria and viruses. Curr. Protoc. Cytom. 11, 1–15.
Mayali, X., et al., 2014. Phylogenetic patterns in the microbial response to resource availability: amino acid incorporation in San Francisco Bay. PLoS One 9 (4), e95842.
Mcmurdie, P.J., Holmes, S., 2012. Phyloseq: A Bioconductor Package for Handling and Analysis of High-Throughput Phylogenetic Sequence Data. Pacific Symposium on Biocomputing.
Metzler, P.M., et al., 1997. New and regenerated production in the South Atlantic off Brazil. Deep Sea Research Part I: Oceanographic Research Papers 44 (3), 363–384.
Milici, M., Tomasch, J., Wos-Oxley, M.L., Wang, H., Jáuregui, R., Camarinha-Silva, A., Deng, Z.-L., Plumeier, I., Giebel, H.-A., Wurst, M., Pieper, D.H., Simon, M., Wagner-Döbler, I., 2016. Low diversity of planktonic bacteria in the tropical ocean. Sci. Rep. 6 (1) https://doi.org/10.1038/srep19054.
Montserrat, F., Guilhon, M., Corrêa, P.V.F., Bergo, N.M., Signori, C.N., Tura, P.M., Santos Maly, M.d.L., Moura, D., Jovane, L., Pellizari, V., Sumida, P.Y.G., Brandini, F.P., Turra, A., 2019. Deep-sea mining on the Rio Grande Rise (Southwestern Atlantic): A review on environmental baseline, ecosystem services and potential impacts. Deep Sea Res. Part I: Oceanographic Res. Pap. 145, 31–58.
Morel, F.M.M., Price, N.M., 2003. The biogeochemical cycles of trace metals in the oceans. Science 300, 944–947.
Morel, F.M.M., Lam, P.J., Saito, M.A., 2020. Trace Metal Substitution in Marine Phytoplankton. Annu. Rev. Earth Planet. Sci. 48 (1), 491–517.
Niner, H.J., Ardron, J.A., Escobar, E.G., Gianni, M., Jaeckel, A., Jones, D.O.B., Levin, L. A., Smith, C.R., Thiele, T., Turner, P.J., Van Dover, C.L., Watling, L., Gjerde, K.M., 2018. Deep-sea mining with no net loss of biodiversity—an impossible aim. Front. Mar. Sci. 5 https://doi.org/10.3389/fmars.2018.00053.
Oksanen, J. et al., 2016. Vegan: community ecology package. R Package 2.3-3, pp. 3.
Orcutt, B.N., Bradley, J.A., Brazelton, W.J., Estes, E.R., Goordial, J.M., Huber, J.A., Jones, R.M., Mahmoudi, N., Marlow, J.J., Murdock, S., Pachiadaki, M., 2020. Impacts of deep-sea mining on microbial ecosystem services. Limnol. Oceanogr. 65 (7), 1489–1510.
Pajares, Silvia, et al., 2019. Molecular and isotopic evidence of the distribution of nitrogen-cycling microbial communities in the oxygen minimum zone of the Tropical Mexican Pacific. FEMS Microbiol. Ecol. 95 (10), fiz143.
Pajares, S., Varona-Cordero, F., Hernández-Becerril, D.U., 2020. Spatial Distribution Patterns of Bacterioplankton in the Oxygen Minimum Zone of the Tropical Mexican Pacific. Microb. Ecol. 80 (3), 519–536.
Parada, A.E., Needham, D.M., Fuhrman, J.A., 2016. Every base matters: assessing small subunit rRNA primers for marine microbiomes with mock communities, time series and global field samples. Environ. Microbiol. 18 (5), 1403–1414.
Partensky, F., Hess, W.R., Vaulot, D., 1999. Prochlorococcus, a marine photosynthetic prokaryote of global significance. Microbiol. Mol. Biol. Rev. 63 (1), 106–127.

Perez, J., dos Santos Alves, E., Clark, M., Bergstad, O.A., Gebruk, A., Azevedo Cardoso, I., Rogacheva, A., 2012. Patterns of life on the southern Mid-Atlantic Ridge: compiling what is known and addressing future research. Oceanography 25 (4), 16–31.
Raven, J.A., 1998. The twelfth Tansley Lecture. Small is beautiful: the picophytoplankton. Funct. Ecol. 12 (4), 503–513.
Rink, B., Seeberger, S., Martens, T., Duerselen C, D., Simon, M., Brinkhoff, T., 2007. "Effects of phytoplankton bloom in a coastal ecosystem on the composition of bacterial communities. Aquat. Microb. Ecol. 48, 47–60.
Rocke, E., Noyon, M., Roberts, M., 2020. Picoplankton and nanoplankton composition on and around a seamount, affected by an eddy dipole south of Madagascar. Deep Sea Res. Part II: Top. Stud. Oceanography 176, 104744. https://doi.org/10.1016/j.dsr2.2020.104744.
Rolinski, S., Segschneider, J., Sündermann, J., 2001. Long-term propagation of tailings from deep-sea mining under variable conditions by means of numerical simulations. Deep Sea Res. Part II: Top. Stud. Oceanography 48 (17-18), 3469–3485.
Salazar, G., Cornejo-Castillo, F.M., Benítez-Barrios, V., Fraile-Nuez, E., Álvarez-Salgado, X.A., Duarte, C.M., Gasol, J.M., Acinas, S.G., 2016. Global diversity and biogeography of deep-sea pelagic prokaryotes. ISME J. 10 (3), 596–608.
Schlitzer, R., 2016. Ocean Data View, version 4.7. 8.
Sheik, C.S., Reese, B.K., Twing, K.I., Sylvan, J.B., Grim, S.L., Schrenk, M.O., Sogin, M.L., Colwell, F.S., 2018. Identification and removal of contaminant sequences from ribosomal gene databases: lessons from the census of deep life. Front. Microbiol. 9 https://doi.org/10.3389/fmicb.2018.0084010.3389/fmicb.2018.00840.s001.
Shulse, C.N., Maillot, B., Smith, C.R., Church, M.J., 2017. Polymetallic nodules, sediments, and deep waters in the equatorial North Pacific exhibit highly diverse and distinct bacterial, archaeal, and microeukaryotic communities. MicrobiologyOpen 6 (2), e00428. https://doi.org/10.1002/mbo3.2017.6.issue-210.1002/mbo3.428.
Silveira, I.C.A., Napolitano, D.C., Farias, I.F., 2020. Water Masses and Oceanic Circulation of the Brazilian Continental Margin and Adjacent Abyssal Plain. Springer, Cham, Brazilian Deep-Sea Biodiversity, pp. 7–36.
Smith, K.L., Ruhl, H.A., Kaufmann, R.S., Kahru, M., 2008. Tracing abyssal food supply back to upper-ocean processes over a 17-year time series in the northeast Pacific. Limnol. Oceanogr. 53 (6), 2655–2667.
Teeling, H., Fuchs, B.M., Becher, D., Klockow, C., Gardebrecht, A., Bennke, C.M., Kassabgy, M., Huang, S., Mann, A.J., Waldmann, J., Weber, M., Klindworth, A., Otto, A., Lange, J., Bernhardt, J., Reinsch, C., Hecker, M., Peplies, J., Bockelmann, F. D., Callies, U., Gerdts, G., Wichels, A., Wiltshire, K.H., Glöckner, F.O., Schweder, T., Amann, R., 2012. "Substrate-controlled succession of marine bacterioplankton populations induced by a phytoplank- ton bloom. Science 336 (6081), 608–611.
Teeling, Hanno, et al., 2016. "Recurring patterns in bacterioplankton dynamics during coastal spring algae blooms. elife 5, e11888.
Unfried, F., Becker, S., Robb, C.S., Hehemann, J.-H., Markert, S., Heiden, S.E., Hinzke, T., Becher, D., Reintjes, G., Krüger, K., Avcı, B., Kappelmann, L., Hahnke, R.L., Fischer, T., Harder, J., Teeling, H., Fuchs, B., Barbeyron, T., Amann, R.I., Schweder, T., 2018. Adaptive mechanisms that provide competitive advantages to marine bacteroidetes during microalgal blooms. ISME J. 12 (12), 2894–2906.
Vandieken, V., Pester, M., Finke, N., Hyun, J.-H., Friedrich, M.W., Loy, A., Thamdrup, B. o., 2012. Three manganese oxide-rich marine sediments harbor similar communities of acetate-oxidizing manganese-reducing bacteria. ISME J. 6 (11), 2078–2090.
Verna, C., Ramette, A., Wiklund, H., Dahlgren, T.G., Glover, A.G., Gaill, F., Dubilier, N., 2010. High symbiont diversity in the bone-eating worm Osedax mucofloris from shallow whale-falls in the North Atlantic. Environ. Microbiol. 12 (8), 2355–2370.
Walsh, E.A., Kirkpatrick, J.B., Rutherford, S.D., Smith, D.C., Sogin, M., D'Hondt, S., 2016. Bacterial diversity and community composition from seasurface to subseafloor. ISME J. 10 (4), 979–989.
Wang, K., Wommack, K.E., Chen, F., 2011. Abundance and distribution of Synechococcus spp. and cyanophages in the Chesapeake Bay. Appl. Environ. Microbiol. 77 (21), 7459–7468.
Wagner-Döbler, I., Biebl, H., 2006. Environmental biology of the marine Roseobacter lineage. Annu. Rev. Microbiol. 60 (1), 255–280.
Wickham, H., 2009. ggplot2: Elegant Graphics for Data Analysis. Springer Publishing Company, Incorporated, New York.
Wedding, L.M., Friedlander, A.M., Kittinger, J.N., Watling, L., Gaines, S.D., Bennett, M., Hardy, S.M., Smith, C.R., 2013. From principles to practice: a spatial approach to systematic conservation planning in the deep sea. Proc. Roy. Soc. B: Biol. Sci. 280 (1773), 20131684. https://doi.org/10.1098/rspb.2013.1684.
Welschmeyer, N.A., 1994. Fluorometric analysis of chlorophyll a in the presence of chlorophyll b and pheopigments. Limnol. Oceanogr. 39 (8), 1985–1992.
Wigham, B.D., Tyler, P.A., Billett, D.S.M., 2003. "Reproductive biology of the abyssal holothurian Amperima rosea: an opportunistic response to variable flux of surface derived organic matter?" Marine Biological Association of the United Kingdom. J. Mar. Biol. Assoc. UK 83 (1), 175–188.
Zubkov, M.V., Fuchs, B.M., Archer, S.D., Kiene, R.P., Amann, R., Burkill, P.H., 2001. "Linking the composition of bacterioplankton to rapid turnover of dissolved dimethylsulphoniopropionate in an algal bloom in the North Sea. Environ. Microbiol. 3 (5), 304–311.